

Reversible wettability of electron-beam deposited indium-tin-oxide driven by ns-UV irradiation

Luana Persano,^{1,2,a)} Pompilio Del Carro,¹ and Dario Pisignano^{1,2,3}

¹NNL, National Nanotechnology Laboratory of CNR-Istituto Nanoscienze, Università del Salento, via Arnesano, I-73100 Lecce, Italy

²Center for Biomolecular Nanotechnologies @UNILE, Istituto Italiano di Tecnologia, Via Barsanti, I-73010 Arnesano-LE, Italy

³Dipartimento di Matematica e Fisica "Ennio De Giorgi," Università del Salento, via Arnesano, I-73100 Lecce, Italy

(Received 27 January 2012; accepted 20 March 2012; published online 12 April 2012)

Indium tin oxide (ITO) is one of the most widely used semiconductor oxides in the field of organic optoelectronics, especially for the realization of anode contacts. Here the authors report on the control of the wettability properties of ITO films deposited by reactive electron beam deposition and irradiated by means of nanosecond-pulsed UV irradiation. The enhancement of the surface water wettability, with a reduction of the water contact angle larger than 50°, is achieved by few tens of seconds of irradiation. The analyzed photo-induced wettability change is fully reversible in agreement with a surface-defect model, and it can be exploited to realize optically transparent, conductive surfaces with controllable wetting properties for sensors and microfluidic circuits. © 2012 American Institute of Physics. [<http://dx.doi.org/10.1063/1.3701590>]

The use of thin films of indium tin oxide [(ITO), In₂O₃:Sn] is widespread in many applications, such as field emission displays,¹ plasma panels,² solar cells,³ organic electroluminescent,⁴ and electrochromic devices.⁵ Among metal-oxide materials, ITO offers a combination of optical and electrical properties which still makes it the material of election for both organic light emitting diodes and organic solar cells. In particular, thin films of ITO are generally characterized by high transparency at visible wavelength (~90%), low resistivity (tens of Ω/□), and high work function (4-5 eV), and they are used as anode contact substrates for optoelectronic devices. In this framework, many applications require the subsequent deposition of thin films of organic materials; therefore, the accurate control of the surface morphology and the wetting properties of the ITO films become very important.

Commonly available ITO substrates, generally made by sputtering, are often characterized by relatively high surface roughness (tens of nm) which may cause problems for a subsequent effective deposition of organics.⁶ In fact, the surface inhomogeneity of underneath ITO films can be subsequently transferred to the layers of active organics, especially when the latter are deposited by spin coating or more broadly by solution casting methods. In a previous paper,⁷ we have reported on the optical and electrical properties of ITO thin films deposited by electron beam evaporation, demonstrating how the surface roughness can be strongly reduced (down to a few nm), still preserving high optical transparency and good conduction properties. In these films, thermal treatments up to 573 K induce modifications both morphologically, inducing grains coalescence and consistently increasing the surface roughness (about 30%), and electronically through a partial redistribution of the electronic states.

Besides roughness, the wettability of ITO critically affects the subsequent deposition of solutions. For instance, higher wettability by aqueous solutions and other polar liquids is also established to improve significantly the performances of organic light-emitting devices.⁸⁻¹¹ Indeed, the surface wettability is an important requirement for the precise thickness control of the deposited layers, a condition which is relevant for the efficient diffusion and the recombination processes occurring within the active materials and determining the device performances, and it is also important to achieve a better adhesion at the anode-organic interface. The water contact angle of commercial ITO substrates typically ranges from 70° to 90°, and usually performed plasma oxygen or UV-ozone treatments significantly increase the surface hydrophilic character but can be quite long (with duration from a few to tens of minutes depending on the processing conditions, RF or UV-irradiation power, etc.).¹²⁻¹⁵ For these reasons, alternative and possibly faster methods to treat ITO and control the film wettability are highly desirable.

In this letter, we report on the rapid wettability enhancement of ITO films made by electron beam evaporation, upon nanosecond UV irradiation at different exposure fluences (up to 25 mJ/cm²). A few tens of seconds of irradiation are enough to reduce the water contact angle by a factor 2.5, without inducing other variations of optical or electrical properties. After overnight storage in dark, the pristine wettability is recovered with a fully reversible behaviour of the ITO surfaces.

Our ITO films are deposited on Corning glass and Si/SiO₂ substrates by reactive electron-beam evaporation. The evaporation chamber is evacuated to a base pressure of 9 × 10⁻⁷ mbar, and the oxygen atmosphere is achieved via a gas inlet with flow of 4-6 sccm. The films are deposited from 99.9% purity In₂O₃:Sn (90 and 10 wt. %, respectively) pieces [IAM (International Advanced Materials), NY] at a working

^{a)}Corresponding author. E-mail address: luana.persano@nano.cnr.it.

pressure of $1\text{--}3 \times 10^{-5}$ mbar, with homogeneous thickness of about 150 nm. During film growth, the chamber temperature is kept at 240 °C by a halogen lamp. The electron-beam source operates at 10 kV, with a constant deposition rate of about 1.0 \AA s^{-1} , monitored by a quartz crystal microbalance. The optical irradiation of the ITO films is performed with a Q-switched Nd-doped yttrium aluminum garnet pulsed laser (Spectra-Physics) emitting at 355 nm, with a pulse duration of 3 ns and a repetition rate of 10 Hz (fluence 0.4–25 mJ/cm², irradiation times 5–60 s). The pump beam is focused on the sample providing a circular spot (diameter, $\phi = 0.9$ cm). The water contact angle is measured with a KSV CAM200 system. Distilled water is dispensed on the sample surface using a microsyringe, with typical drop volumes of about 3 μ L. The morphological characterization of the ITO surfaces is carried out before and after UV irradiation by scanning electron microscopy (SEM) and by contact mode atomic force microscopy (AFM) in air with a Nanoscope III controller with a Digital Instruments Multimode head. All measurements are performed under ambient conditions.

Fig. 1 shows the behaviour of the static contact angle of ITO samples (full circles), deposited at 3×10^{-5} mbar pressure, upon ns-pulsed irradiation for 30 s at different fluences. The water contact angle of the as-deposited films is 86° (top inset in Fig. 1), and it monotonically decreases to 35° (bottom inset) upon increasing the laser fluence up to 25 mJ/cm². ITO samples grown at different oxygen partial pressures show an analogous behaviour. Optical and electrical characterizations performed before and after irradiation do not evidence significant variations in the properties of the samples, showing a sheet resistance of $(18 \pm 2) \text{ \Omega}/\square$ and transmittance maxima above 90% (Fig. 2(a)). SEM and AFM images, displayed in Figs. 2(b)–2(e), show the typical grain distribution of as-deposited ITO films,^{13,16} which exhibit an average grain size (80 ± 25) nm, height ($\cong 30$ nm), and mean surface roughness ($\cong 9$ nm). These values do not exhibit appreciable variations upon UV irradiation (10 mJ/cm² for 30 s, Fig. 2(e)).

In addition, the morphological inspection allows to appreciate the sequential growth behaviour of ITO grains

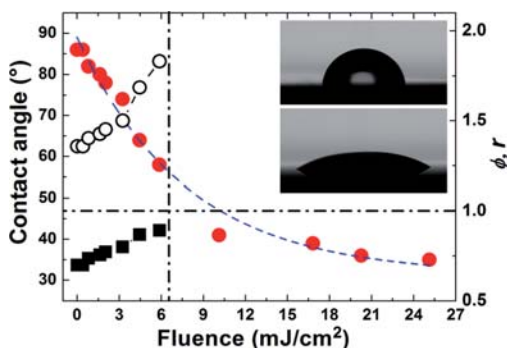


FIG. 1. Behaviour of the static contact angle (full dots, left vertical scale) vs ns UV-irradiation fluence (irradiation time = 30 s). Right scale: corresponding Φ (full squares) and r (empty dots) parameters according to the modified Wenzel model. The dashed lines superimposed to data are guides for the eye. The horizontal dash-dotted line indicates the maximum, unity theoretical value of Φ . Data at the right of the vertical dash-dotted line can not be described by the model. Insets: photographs of water drops on as-deposited (top inset) and UV-irradiated (at 25 mJ/cm², bottom inset) ITO surfaces.

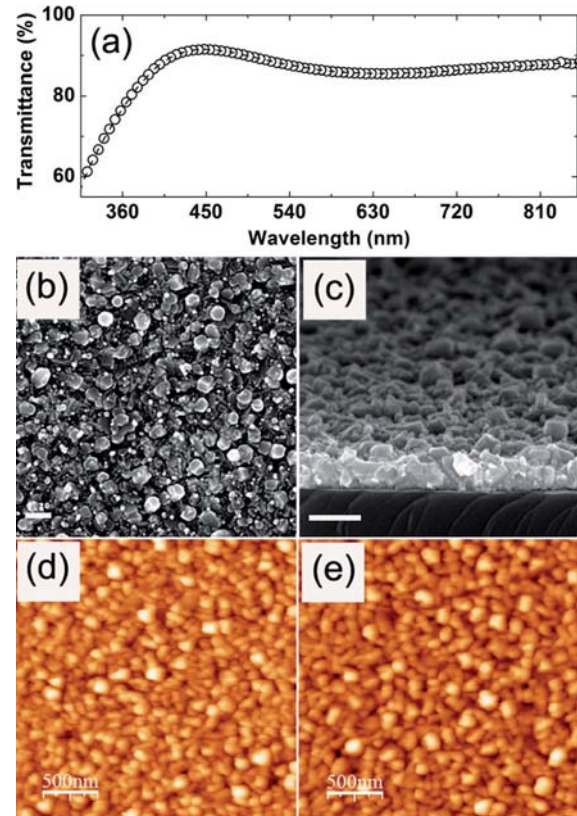


FIG. 2. (a) Transmittance spectra of as-deposited ITO films (dashed line) and after irradiation (open dots) at 10 mJ/cm² for 30 s. Top (b) and cross-sectional (c) SEM images of as-deposited ITO films. Scale bars = 200 nm. AFM micrographs of as-deposited ITO films (d) and after irradiation (e) at 10 mJ/cm² for 30 s.

through the coexistence of a multi-lengthscale roughness, with the formation of sub-20 nm clusters decorating the main grains. The effect of the roughness on the wettability can be explained by different theories, accounting for the complete penetration of the liquid drop within the structured solid as in the Wenzel model,¹⁷ and vice versa, for droplets standing on the top of the solid features with air trapped in the recessed regions of the pattern, which is described by the Cassie-Baxter model.¹⁸ In general, the presence of air pockets beneath the liquid drop is expected to be disfavoured for hydrophilic materials and the investigation of the transition between the Wenzel and the Cassie states in case of complex surface with inhomogeneous and periodic roughness is still an open field.^{19,20} In particular, we suggest that the behaviour of pristine ITO surfaces can be explained by considering drops in an intermediate state, with the liquid *partially* penetrating into the solid features, leaving incomplete unwetted fractions underneath.²¹ The existence of local energy minima of the liquid-air interface within the structured features could explain the gradual transition from the Cassie-Baxter to the Wenzel state.²² This intermediate state is schematized in the inset of Fig. 3(a) and described by a modified Wenzel model,²³ where the surface displacement of the liquid-gas interface by an amount, ΔA , determines a change in surface free energy, ΔF , which is given by

$$\Delta F = (\gamma_{SL} - \gamma_{SV})r\Phi\Delta A + \gamma_{LV}(1 - \Phi)\Delta A + \gamma_{LV}\cos\Theta\Delta A. \quad (1)$$

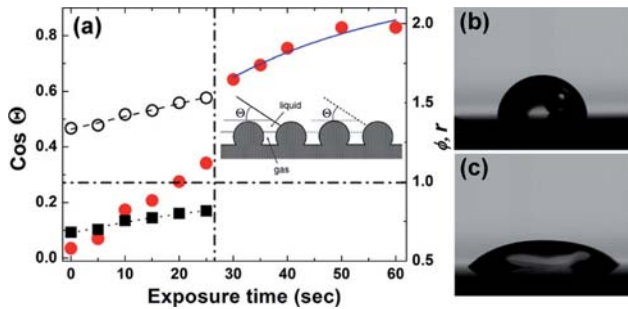


FIG. 3. (a) Static contact angle vs ns UV-irradiation time (full dots, left vertical scale), at an exposure fluence of 10 mJ/cm^2 . Right scale: corresponding Φ (full square) and r (empty dots) parameters according to the modified Wenzel model. Dashed and dotted lines superimposed to data are guides for the eye. The continuous line for times $\geq 30 \text{ s}$ is the exponential fit to experimental data, according to a forward hydrophilic reaction rate model. Dash-dotted lines as in Fig. 1. Inset: schematics of the partial penetration of the liquid within the recessed features of the surface. (b), (c) Photographs of water drops residing on the initial (a) and UV-irradiated (b) ITO surfaces. Irradiation time = 60 s.

In the previous expression γ_{SL} , γ_{SV} , and γ_{LV} are the solid-liquid, solid-vapor, and liquid-vapor interfacial tensions, respectively, Θ indicates the contact angle on the rough surface, $r > 1$ is the surface ratio, namely the overall area of the wetted surface projected on the horizontal plane of the solid, and $\Phi < 1$ indicate the wetted fraction of the solid. According to Eq. (1), in absence of surface energy variations, the equilibrium contact angle is related to that ($\Theta_0 = 67^\circ$) for a very smooth ITO (Ref. 24) and to the surface topology by

$$\cos\Theta = r\Phi\cos\Theta_0 - (1 - \Phi). \quad (2)$$

This model describes well as-deposited ITO surfaces. Schematizing grains as fragments of spheres with diameter given by the average value (80 nm) estimated by AFM analysis, with our geometry and contact angle values for pristine ITO we obtain $r \cong 1.4$ and $\Phi \cong 0.7$, respectively. Upon UV irradiation by fluences above 6 mJ/cm^2 (Fig. 1) or for times longer than 25 s at 10 mJ/cm^2 (Fig. 3(a)) the contact angle behaviour can be still described by Eq. (1), that however provides a physically possible behaviour of r (open circles) and Φ (full squares) only for irradiated surfaces with $\Theta > 50^\circ$. For lower angles, the modified Wenzel model does not provide real solutions for r and Φ . Consequently, not only the topography but also the photochemistry at the surface should be taken into account to explain the wettability changes after UV-exposure. To investigate the wettability dynamics more in depth, we also measure the contact angle varying the exposure time at a fixed fluence of 10 mJ/cm^2 . Increasing the exposure time by steps of 5 s we observe a monotonous decrease of the contact angle down to 34° within the first 50 s and then a saturation (Fig. 3). This behaviour can be explained by taking into account surface energy variations upon UV exposure. In fact, the force balance among the interfacial tensions of a liquid drop lying on the surface generally leads to $\cos\Theta = r\Phi$ $[(\gamma_{SV} - \gamma_{SL})/\gamma_{LV}] - (1 - \Phi)$. This expression can be developed by considering a linear relation between the interfacial tension ratio and the more hydrophilic surface fraction (c), i.e., $(\gamma_{SV} - \gamma_{SL})/\gamma_{LV} = f_1c + f_2$, where f_1 and f_2 are constants, and a single rate equation for the temporal dynamics of c (Ref. 25)

$$\frac{\partial c(t)}{\partial t} = k_W(1 - c), \quad (3)$$

where k_W is the forward hydrophilic reaction rate constant, and the backward reaction rate is neglected under exposure conditions. This finally provides for the contact angle the following temporal dependence

$$\cos\Theta = r\Phi f_1 \{1 - [1 - c(t=0)]e^{-k_W t}\} + r\Phi f_2 - (1 - \Phi), \quad (4)$$

which fits well experimental data for $\Theta < 50^\circ$, corresponding to irradiation times longer than 30 s (continuous fitting line in Fig. 3), with $k_W \cong 3 \times 10^{-2} \text{ s}^{-1}$. This value is at least six time higher than in previously studied hydrophilic conversion processes by continuous irradiation.²⁵

In the last few years, the wettability enhancement and conversion properties of ceramics and oxides under UV irradiation have been largely investigated.²⁶ Many studies have been focused on Titanium and Zinc Oxide as continuous films or nanostructures^{27–29} and recently on the photo-conversion capability of wires and rods made of indium oxide (In_2O_3)³⁰ and tin oxide (SnO_2).³¹ While for nanostructures the surface morphology plays an important role, in case of films the photo-generation of surface electron-hole pairs that can react with lattice oxygen to form surface oxygen vacancies is thought to make the major contribution to the wettability change phenomena, which are quite similar in different oxide species.^{27,32} In fact, photogenerated oxygen vacancies at the surface can originate preferential adsorption of water molecules at the defect sites. Such a surface-defect model agrees well with the here observed increase of the hydrophilic behaviour upon UV-irradiation, which is largely independent on the surface morphology while displaying a clear dependence on both the irradiation fluence and the exposure time. A further confirmation of these conclusions comes since the photogenerated hydrophilic condition reconverts to its original state. Following ns-irradiation, storing ITO films overnight in dark under ambient conditions allows to observe a clear reversibility of the wettability ns-photo-enhancement, as tested for many cycles without significant fatigue effects (Fig. 4). This effect is attributed to the

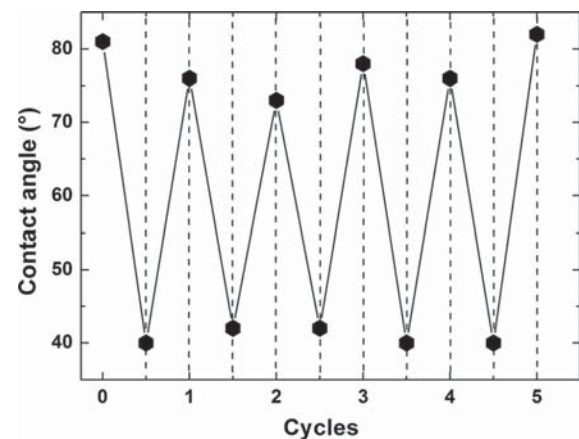


FIG. 4. Contact angle cycles. Each cycle includes irradiation at 10 mJ/cm^2 for 30 s and one night of storage in dark.

adsorption dynamics of hydroxyls on the defect sites, which are gradually replaced by oxygen in the air.³¹

In conclusion, we demonstrate ns-UV irradiation as effective and fast method to change the surface wettability of ITO films. By irradiating for a few seconds electron-beam deposited ITO films with ns-UV pulsed laser, the water contact angle is reduced by more than 50°. The wettability is changed by varying both the irradiation time and the fluence, with the most hydrophilic state ($\Delta\theta \cong 35^\circ$) reached within 30 s at 25 mJ/cm². The photochemistry effects of the ns-irradiation are fully reversible and the surface wettability reconvert to the initial state after overnight storage. The control and reversible cycling of wettability can be exploited in many applications, including microfluidics and switching surfaces³³ in optically transparent lab-on-chips, and patterned organic optoelectronic devices.³⁴

We thank Dr. Giovanni Potente for SEM measurements and Dr. A. Cannavale for assistance in electrical measurements.

¹C.-C. Kao and Y.-C. Liu, *Mat. Chem. Phys.* **115**, 463 (2009).

²C.-H. Moon, *Displays* **31**, 175 (2010).

³M. C. Gather, A. Köhnen, A. Falcou, H. Becker, and K. Meerholz, *Adv. Funct. Mater.* **17**, 191 (2007).

⁴M. Helgesen, R. Søndergaard, and F. C. Krebs, *J. Mater. Chem.* **20**, 36 (2010).

⁵S. Koyuncu, O. Usluer, M. Can, S. Demic, S. Iclib, and N. S. Sariciftci, *J. Mater. Chem.* **21**, 2684 (2011).

⁶J. Lukkari, M. Alanko, L. Heikkilä, R. Laiho, and J. Kankare, *Chem. Mater.* **5**, 289 (1993).

⁷F. Matino, L. Persano, V. Arima, D. Pisignano, R. I. R. Blyth, R. Cingolani, and R. Rinaldi, *Phys. Rev. B* **72**, 085437 (2005).

⁸J. S. Kim, R. H. Friend, and F. Cacialli, *J. Appl. Phys.* **86**, 2774 (1999).

⁹Y.-C. Chen, P.-C. Kao, Y.-C. Fang, H.-H. Huang, and S.-Y. Chu, *Appl. Phys. Lett.* **98**, 263301 (2011).

¹⁰Z. H. Huang, X. T. Zeng, X. Y. Sun, E. T. Kang, J. Y. H. Fuh, and L. Lu, *Org. Electron.* **9**, 51 (2008).

¹¹P. Vacca, M. Petrosino, A. Guerra, R. Chierchia, C. Minarini, D. Della Sala, and A. Rubino, *J. Phys. Chem. C* **111**, 17404 (2007).

¹²S. K. So, W. K. Choi, C. H. Cheng, L. M. Leung, and C. F. Kwong, *Appl. Phys. A* **68**, 447 (1999).

¹³P. Svarnas, L. Yang, M. Munz, A. J. Edwards, A. G. Shard, and J. W. Bradley, *J. Appl. Phys.* **107**, 103313 (2010).

¹⁴L. Yang, A. G. Shard, J. L. S. Lee, and S. Ray, *Surf. Interf. Anal.* **42**, 911 (2010).

¹⁵M. C. Gather, A. Köhnen, A. Falcou, H. Becker, and K. Meerholz, *Adv. Funct. Mater.* **17**, 191 (2007).

¹⁶Y.-C. Park, Y.-S. Kim, H.-K. Seo, S. G. Ansari, and H.-S. Shin, *Surf. Coat. Technol.* **161**, 62 (2002).

¹⁷R. N. Wenzel, *Ind. Eng. Chem.* **28**, 988 (1936).

¹⁸A. B. D. Cassie and S. Baxter, *Trans. Faraday. Soc.* **40**, 546 (1944).

¹⁹N. A. Patankar, *Langmuir* **20**, 7097 (2004).

²⁰A. Lafuma and D. Quéré, *Nat. Mater.* **2**, 457 (2003).

²¹N. J. Shirtcliffe, G. McHale, M. I. Newton, and C. C. Perry, *Langmuir* **21**, 937 (2005).

²²M. E. Abdelsalam, P. N. Bartlett, T. Kelf, and J. Baumberg, *Langmuir* **21**, 1753 (2005).

²³V. Zorba, L. Persano, D. Pisignano, A. Athanassiou, E. Stratakis, R. Cingolani, P. Tzanetakis, and C. Fotakis, *Nanotechnology* **17**, 3234 (2006).

²⁴Z. Z. You, *Mater. Lett.* **61**, 3809 (2007).

²⁵K. Seki and M. Tachiya, *J. Phys. Chem. B* **108**, 4806 (2004).

²⁶I. P. Parkin and R. G. Palgrave, *J. Mater. Chem.* **15**, 1689 (2005).

²⁷R.-D. Sun, A. Nakajima, A. Fujishima, T. Watanabe, and K. Hashimoto, *J. Phys. Chem. B* **105**, 1984 (2001).

²⁸J. Han and W. Gao, *J. Electron. Mater.* **38**, 601 (2009).

²⁹Q. Zhou, X. Yang, S. Zhang, Y. Han, G. Ouyang, Z. He, C. Liang, M. Wu, and H. Zhao, *J. Mater. Chem.* **21**, 15806 (2011).

³⁰G. Shen, B. Liang, X. Wang, H. Huang, D. Chen, and Z. L. Wang, *ACS Nano* **5**, 6148 (2011).

³¹W. Zhu, X. Feng, L. Feng, and L. Jiang, *Chem. Commun.* 2753 (2006).

³²S. Wang, X. Feng, J. Yao, and L. Jiang, *Angew. Chem. Int. Ed.* **45**, 1264 (2006).

³³D. Pisignano, F. Di Benedetto, L. Persano, G. Gigli, and R. Cingolani, *Langmuir* **20**, 4802 (2004).

³⁴J. Z. Wang, Z. H. Zheng, H. W. Li, W. T. S. Huck, and H. Sirringhaus, *Nat. Mater.* **3**, 171 (2005).